SHOCK VAPORIZATION AND THE ACCRETION OF THE ICY SATELLITES OF JUPITER AND SATURN

Thomas J. Ahrens and John D. O'Keefe

Seismological Laboratory, California Institute of Technology,

Pasadena, CA 91125

Abstract. Shock wave data, thermodynamic and phase diagram data for ice, porous ice, and water are taken together with a Rice-Walsh-Bakanova equation of state to define the shock pressures and impact velocities required to induce incipient melting (IM) (6 GPa), complete melting (CM) (10 GPa), and passage through the vapor-liquid critical point (CP) upon isentropic release (22.5 GPa). Upon expanding along the isentrope which passes through CP ~0.5 mass fraction vaporization occurs until a pressure of ~61 kPa (61 mbar) is achieved. Below this pressure ice sublimates and ~0.4 mass fraction H_2O gas is in equilibrium with ice I. The minimum impact velocity required to induce IM, CM, and isentropic release through CP is 2.1, 3.0, and 4.5 km/sec for silicate impactors. For icy projectiles Hugoniot states depend only weakly on initial temperature of ice. The IM, CM, and CP isentropes are achieved upon impacting an icy surface at velocities 3.4, 4.4, and 7.2 km/sec, respectively. We observe that a partial H_2O pressure below 61 kPa and temperatures below 273K, ice partially vaporizes and requires 2800 kJ/kg, of heat of vaporization for complete sublimation. We examine the hypothesis that the smaller satellites of Saturn having mean densities in the 1.1 to 1.4 Mg/m^3 range represent primordial accreted planetesimal condensates (60% (wt.) H_2O, and 40% (wt.) silicate) formed in the proto-Jovian and Saturnian accretionary planetary discs. These densities are in the range expected for water-ice/silicate mixtures constrained to the solar values of O/Si

and O/Mg atomic ratios. We demonstrate that if the large satellites accreted from the same group of planetesimals which formed the small Saturnian satellites impact vaporization of water upon accretion in a porous regolith, at low H_2O partial pressure, can account for the increase in mean planetesimal density from 1.6 Mg/m^3 (43% H_2O + 57% silicate) to a mean planetary density of 1.9 Mg/m^3 for Ganymedean-sized water-silicate objects. If impact volatilization of initially porous planetesimals is assumed, we demonstrate that starting with planetesimals composed of 54% H_2O and 40% silicate (1.35 Mg/m^3) partial devolatilization upon accretion will yield a Ganymede-sized planet, having a radius of 2600 km and a density of 1.85 kg/m^3, similar to that of Ganymede, Callisto, and Titan.

1. INTRODUCTION

We apply knowledge of the properties of water and ice over a wide range of pressures and temperatures and describe constraints on the shock vaporization processes for water and ice in the solar system. In particular, we examine the role of impact vaporization acting during the formation of the Jovian and Saturnian satellites in an attempt to explain the observed density in terms of composition of these rock and ice objects. The imaging instruments on the Voyager I and II spacecraft (Smith et al., 1979a,b, 1981, Morrison, 1982) have provided definitive knowledge of the volumes, and hence, densities, as well as, the surface characteristics of at least 12 satellites of Jupiter and Saturn having planetary radii $\gtrsim$ 100 km (Table 1).

Pollack and Reynolds (1974), and more recently, Lunine and Stevenson (1982), and Pollack and Finale (1982) have discussed the origin of the larger Jovian satellites within a framework of condensation from a "protostellar" disc of

gaseous and particulate material rotating around a newly formed proto-Jupiter (of approximately solar composition). This disc is much like the larger scale protosolar disc from which the sun and the planets themselves form. Like the solar system, itself, this type of model of the Jovian satellite system implies a higher temperature close to Jupiter and thus ultimately less relative condensation of volatiles (e.g. H_2O, NH_3) in the satellites close to the planet as compared to the outer satellites. The Jovian system clearly suggests such a formational history, as the inner satellites (Amalthea, Io, and Europa) have higher mean densities, 3.0 to 3.6 Mg/m^3, and in an analogy to the terrestrial planets) contain a higher fraction of silicates than do the outer larger (lower density) satellites (Ganymede and Callisto). The latter have densities of 1.8 to 1.9 Mg/m^3 (Fig. 1). In such formation models of the Jovian satellites, it is usually assumed that these accreted from small solid objects which formed via gravitational or other instabilities in the proto-Jovian disc. The inner satellites accumulated lower inventories of volatiles as a result of either or both of the following two effects:

(1) Because of the higher temperatures in the vicinity of the early Jupiter, relatively less volatiles can condense. For example, in the Lunine and Stevenson model the temperatures and pressures at the orbits of Amalthea and Callisto are 1350K and 13 MPa and 150K and 0.01 MPa, and

(2) Because the Keplerian velocity around Jupiter of the proto-satellites and hence the speed with which they overtake and accrete smaller solid objects imbedded in the gaseous nebula have a lower encounter velocity with increasing radius from Jupiter, less impact vaporization can occur during accretion.

Whereas the "miniature solar system" model for the Jovian satellite system which has relatively more volatile material condensing with increasing radius in one form or other should be successful in explaining the high density inner satellites versus the low density outer satellites. In the case of the Saturnian

system, the satellite mean density versus radius from the planet relation is irregular. As can be seen in Fig. 1, there is no obvious correlation of mean satellite density with orbital radius.

Examination of Table 1 suggests that one could classify the Jovian and Saturnian satellites into three groups according to mean density: silicate (sil), primordial (p), and partially devolatilized (pd) (e.g. Cole, 1984). By silicate density we mean the density of terrestrial planetary mantles 3-3.5 Mg/m^3. An estimate of a primordial density can be obtained by assuming the solar O/Si atomic ratio of 15.5 (Ross and Aller, 1976). We assume that this ratio determines the abundance of H_2O which is in turn controlled by the abundance of oxygen relative to silicon and hence the abundance of Si. For example, if we consider SiO_2 as being controlled by the abundance of Si then we infer that an atomic ratio is required of 5.16 moles of H_2O to 1 mole of SiO_2. This ratio thus implies a density of 1.23 Mg/m^3 for a water-ice and quartz mixture. Assuming that the most abundant anhydrous silicate in the solar system is probably enstatite $MgSiO_3$ and utilizing the solar atomic ratio of O/Mg of 17.38 and assuming the H_2O/MgO ratio controls the density of primordial low temperature volatile-silicate condensate mixture, a density of 1.08 Mg/m^3 is inferred by the same reasoning. The additional small amounts of oxidized iron will, of course, increase this density. We assume that densities in the above range, correspond to a silicate plus some oxidized iron plus volatile primordial condensate and this is assumed to be representative of densities of the group of the smaller satellites in the Saturnian systems indicated by p.

In the present paper we first examine the shock wave and phase diagram data for water, solid and porous water-ice and define the impact velocity required for shock-induced melting and vaporization of water and ice at various temperatures.

We then examine a possible model of accretion of icy satellites which predicts that the amount of ice devolatilization is related to planetary size. The Lunine and Stevenson (1982) model, predicts final satellite density on the basis of differing environment for accretion as a function of satellite radius from Jupiter. We assume all the satellites in the Jovian and Saturnian system (except J5, J1, and J2) accreted from the same composition of planetesimal material and that the least affected samples of these planetesimals are the smaller satellites of Saturn and possibly also the ring materials of both planets. The partially devolatilized satellites whose density we attempt to predict (Ganymede, Callisto, and Titan) are then assumed to be partially devolatilized, indicated as p.d. in Table 1.

2. Shock Wave Equation of State and Thermodynamic Data for Water, Water-Ice, and Porous Ice.

We need to combine knowledge of the Hugoniot curves for ice targets and the calculated release isentrope curves to determine the impact velocities required to generate sufficient entropy to melt and vaporize ice. The train of logic is as follows:

(a) Given the measured Hugoniot shock velocity, U_s, versus particle velocity, u_p, data, shock pressure versus shock particle velocity curves may be constructed. These allow prediction via the impedance match method (McQueen et al., 1970) of the peak shock pressures induced upon impact of a specific projectiles (e.g. rock or ice) against solid or porous ice or water targets. The amount of material subjected to this peak pressure is in the order of 10^0 to 10^1 times the projectile mass (O'Keefe and Ahrens, 1977).

(b) The single shock data must then be combined with data obtained by double shocking water and/or porous ice to the same pressure but at lesser and

greater temperatures (and hence lesser and greater specific volumes) as well as thermodynamic data to calculate the isentropes in pressure-volume temperature space. The tactic we employed is that of Ahrens and O'Keefe (1972). We utilize pressure volume-entropy-enthalpy data at a single moderate pressure (1 GPa) and increasing (high) temperatures to define a series of states with increasing entropy to specify the foot of isentropes.

(c) These isentropes are then projected to higher pressures using a complete equation of state formalism like that proposed by Bakanova et al. (1976). Once the intersection with the water and ice Hugoniots are found we can infer from the intersection of the various isentropes with the Hugoniot the entropy along the Hugoniot and hence determine from a given shock state whether the entropy density is sufficiently high such that upon pressure release shock induced melting of vaporization will occur. Of special interest are the isentropes that cross the Hugoniot which define the shock pressures required to just produce incipient melting (IM), complete melting (CM), and bring water to the liquid-vapor (steam) critical point (CP).

(d) When the calculated release isentropes are taken together with the low pressure thermodynamic data for the water-ice steam system, as for example, summarized in the form of a Mollier diagram (Bosnjakovic et al., 1970) the mass fraction of vapor produced by a given entropy density as a function of partial pressure of water vapor in the planetary environment may be inferred.

(1) Shock wave data.

Because ice covers the surface of more than 20 of the Jovian and Saturnian satellites (except for J_5, J_1, and S_8) and is a major constituent of the interior of these objects (and it of course covers 70% of the earth) it is important to determine the projectile impact velocities and hence shock pressures required to induce melting and/or vaporization.

The available Hugoniot data for water-ice and porous-ice in terms of shock velocity, U, particle velocity, u, relations of the form

$$U = C_o + \lambda_1 u + \lambda_2 u^2 \quad (1)$$

is given in Table 2. Shock pressure and shock density (or specific volume, V) can be obtained from the constants in Table 2 via the Rankine Hugoniot shock equations for pressure, P, density, ρ, and internal energy, E, or enthalpy, H, respectively.

$$P - P_o = \rho_o u U \quad (2)$$

$$\rho = \rho_o U/(U-u) \text{ or } V = V_0 (U-u)/U \quad (3)$$

$$E - E_o = (P_o+P)(V_{00}-V)/2 \text{ or } H - H_o = (P_o+P)(V_{00}+V)/2 \quad (4)$$

In equations 2-4, P_o, ρ_o, V_0, E_o, and H_o are the crystal density, specific crystal volume, internal energy and enthalpy in the initial state. In the present paper, energies and enthalpies (and entropy) are measured relative to conditions at 1 bar and 0K. V_{00} is the pre-shock initial specific volume which in the case of porous ice will be greater than V_0. For no porosity $V_0 = V_{00}$. In the case of liquid water, the shock wave data are described via a set of bilinear equations by Mitchell and Nellis (1982) who assume a high pressure regime extending from 4.4 to 83 GPa and Bakanova et al. (1976) who defined the high pressure regime from 8 to 55 GPa. Double (reflected) shock experiments on water have also been carried out by Walsh and Rice (1957), Bakanova et al. (1976), and Mitchell and Nellis (1982), the latter to peak pressures of 230 GPa. In addition, a large number of shock wave data for solid ice initially at temperatures of 258 to 263 K are available over a pressure range from 0.6 to 50.3 GPa (Fig. 2). These data are also closely fit by a linear shock velocity-particle velocity relation. Below 3 GPa,

shock waves in solid ice demonstrate interesting structure involving intermediate shock states due to phase transitions. These are described by Gaffney (1984) in this volume.

When the final shock state data summarized in Table 2 is cast into the pressure-particle velocity plane (Figure 3) via equation 2, it can be seen that liquid water (on account of its greater density) initially has a slightly higher shock impedance (larger value of shock pressure at a fixed particle velocity) than ice and that this small impedance contrast reverses (on account of more shock heating in ice) above ~95 GPa at a particle velocity of 7.7 km/sec. Porous ices with lower initial densities have correspondingly lower shock impedance.

The representation of Hugoniot curves in the pressure-particle velocity plane via the impedance match method (McQueen et al., 1970) allows straightforward determination of projectile-target peak shock pressures from the impact velocities. To demonstrate how this is carried out we indicate in Fig. 2 the escape velocity of water-bearing objects in the solar system along the abscissa (from 0.16 km/sec for Mimas to 11.19 km/sec for the earth). In general, the infall velocity is the minimum velocity for which a projectile can impact the planetary surface in the case where no atmosphere exists or the projectile is large enough not to be affected by its passage through the atmosphere. This minimum velocity then can be increased substantially in the case of the satellites of the major planets by the following three factors which are listed in order of importance.

(1) The effect of gravity focusing by the mass of the planet.

(2) The effect of heliocentric velocity of the planet, and

(3) The effect of the orbital velocity about the planet.

The effect of gravitational focusing by the high infall velocity (escape velocity of Jupiter and Saturn, 60 and 36 km/sec, respectively) of objects on their

planetary satellites is demonstrated with the mean impact velocity and flux concentrations given in Table 3. Table 3 assumes that for the Jovian system objects have a mean encounter velocity of 8 km/sec. At Jupiter's heliocentric distance many of these objects are cometary (see Shoemaker and Wolf, 1982).

The pressure-particle velocity Hugoniot of the impactors is plotted backward centered at the impact velocity. Thus shown in Fig. 2, a projectile impacting at 11.19 km/sec having the pressure-particle velocity characteristics of serpentinite, will induce a shock pressure of 41, 63, 90, and 90.5 GPa in 0.35 and 0.6 Mg/m^3 porous ice, solid ice, and water, respectively. In contrast to the major and terrestrial planets the minimum infall velocities of the Jovian and Saturnian satellites are much lower as indicated in Fig. 3. For solid ice infalling at the escape velocity of Ganymede (2.74 km/sec) a peak pressure of only 4.2 GPa is induced in the projectile and target.

(2) Equation of state for water and ice.

It was recognized as early as 1957 when Rice and Walsh (1957) carried out the first extensive analysis of single and reflected shock data for water that the formulation of a complete thermal equation of state according to the Mie-Gruneisen equation --- so effective for metals (e.g. Rice et al., 1957) was infeasible for application to water and other molecular fluids. Instead Rice and Walsh proposed on the basis of a series of reflected shock data in which different enthalpy states were achieved at a given pressure that the thermodynamic quantity $(\partial H/\partial V)_P$ depends strongly on P (and is effectively independent of V or T at constant P). They then defined a thermodynamic quantity ξ (P) which we will all the Rice-Walsh parameter, as

$$\xi(P) \equiv C_p/(\partial V/\partial T)_P = \left[\frac{\partial H}{\partial T}\right]_P \Big/ \left[\frac{\partial V}{\partial T}\right]_P \qquad (5)$$

Eq. (5) is analogous to the Mie-Gruneisen equation of state, where a state at a given E can be calculated for a given pressure, P, by comparing it to the internal energy (E_r), and pressure (P_r) at the same volume V. Here E_r and P_r refer to the reference thermodynamic path such as the principal Hugoniot. The Mie-Gruneisen equation-of-state is written as:

$$E = E_r + V/\gamma\,(P-P_r) \tag{6}$$

where

$$\gamma \equiv V\,(\partial P/\partial E)_v \tag{7}$$

In analogy with the Mie-Gruneisen parameter, the Rice-Walsh parameter is used to relate enthalpy H and volume, V, at the same pressure, P, to that along the reference path. The reference path chosen here is the principal Hugoniot of water denoted by the subscript 1. Thus the Rice-Walsh equation is

$$H(P, V) = H_1\,(P) + \xi(P)\,[V-V_1(P)] \tag{8}$$

This treatment satisfactorily describes the available Hugoniot and reflected shock data to 25 GPa and is also concordant with static compression data for water at high temperature as well as high pressure and relatively low temperature on the properties of steam. Upon obtaining additional reflected shock data to 120 GPa and porous ice Hugoniot data, Bakanova et al. (1976) utilized an equivalent and more convenient relation than equation 8 specifying internal energy at constant pressure. The Bakanova et al. parameter is defined as

$$\eta\,(P) \equiv P\,(\partial V/\partial E)_P \tag{9}$$

and is related to the Rice-Walsh parameter by applying the relation

$$(\partial H/\partial V)_P = (\partial E/\partial V)_P + P \tag{10}$$

to obtain

$$\eta\,(P) = P/(\xi - P) \tag{11}$$

From equation 9 it follows that

$$E(P, V) - E_1(P) = \frac{P}{\eta(P)}(V - V_1(P)) \tag{12}$$

where E_1 and V_1 are again the reference internal energy and volume at pressure, P.

To obtain an equation for an isentrope we substitute for $E_1\,(P)$

$$E_1 = E_o + (V_o - V)\,P/2 \tag{13}$$

using the Rankine Hugoniot energy equation (relative to the internal energy, E_0 at STP) into equation 12 and solve for V. This yields

$$V = V_1\,(1+\eta/2) - \eta \left\{ \int_{V_{io}}^{V} PdV - E_{io} + E_o + PV_0/2 \right\} / P \tag{14}$$

where we have also substituted for E

$$E = -\int_{V_{io}}^{V} PdV + E_{io} \tag{15}$$

Here V_{io} and E_{io}, and T_{io} are the specific volume internal energy and temperature state which defines the foot of the isentrope at pressure P_{io}.

An equation for the temperature along the isentrope can be obtained from the differential relation

$$0 = TdS = T\,(\partial S/\partial T)_P\,dT + T\,(\partial S/\partial P)_T\,dP \tag{16}$$

substituting in the first and second term, respectively, and using the

thermodynamic relations

$$C_P/T = (\partial S/\partial T)_P \tag{17a}$$

$$(\partial S/\partial P)_T = -(\partial V/\partial T)_P \tag{17b}$$

yields the differential equation

$$dT/T = dP(\partial V/\partial T)_P/C_P \tag{18}$$

which upon substituting for ξ (P) from equation 8 and integrating yields

$$T_a = T_{io} \exp \int_{P_{io}}^{P} \frac{dP}{\xi(P)} = T_{io} \exp \int_{P_{io}}^{P} \frac{\eta dP}{(1+\eta)} \tag{19}$$

In order to calculate the P-V-T-E isentropic path from equation 14 and 19 the function ξ(P) or η(P) must be determined. Rice and Walsh examined four reflected shock data to 23.5 GPa and fit these to

$$\log_{10} \xi = 1.17943 + 0.030338\ P(GPa) \tag{20}$$

whereas Bakanova et al. fit both porous ice data and water double shock data and fit these to the relation

$$\eta\ (P)\ GPa = 0.07\ [1-\exp(-0.08436P)] + 0.044095P \exp\ (-0.048202\ P) \tag{21}$$

As can be seen in Fig. 4 the η(P) function from both studies are similar. The peak in η in the 15 to 20 GPa range is attributed to the increase pressure-induced ionization which occurs in water and is reflected in the rapid increase in electrical conductivity (Mitchell and Nellis, 1982) of shocked liquid water. To further demonstrate the adequacy of the Bakanova equation of state in describing the thermodynamic properties of water to high pressures, we apply it to calculating shock temperatures for water. Comparison of calculated and measured

shock temperatures is carried out in Appendix A.

In order to calculate the specific release isentrope P-V paths for H_2O other than the paths given by Bakanova (1976), Fig. 5, we can utilize both the phase diagram of water (Fig. 6) and the Mollier diagram (Fig. 7). The phase diagram of water sketched in Fig. 6 demonstrates that upon shocking either liquid water or ice above ~20 GPa it achieves states above the vapor-liquid critical point (647K, 22.1 MPa, 3.1 m^3/Mg). It should be noted that a well-defined critical shock pressure marking the onset of incipient vaporization occurs upon shock release cannot be given. Shock-induced vaporization depends strictly on the partial pressure of H_2O in the environment into which shocked water or ice expands. If the partial pressure of H_2O is sufficiently low (below the ice-I vapor or liquid phase line) shocked water ice will always be vaporized upon sufficient entropy input.

The existence of the ice I-liquid-vapor triple point at 273K and 6.108 kPa implies that shocked ice need not melt first but can bypass the liquid field and sublimate provided the pressure is below the ice I-sublimation line which is given explicitly in Dorsey (1940) as

$$\log_{10} P\,(\text{torr}) = -\frac{2445.5646}{T(K)} + 8.2312 \log_{10} T - 1677.006\,(10^{-5})\,T + \qquad (22)$$

$$120514\,(10^{-10})\,T^2 - 6.757169$$

The Mollier diagram for water, ice, and steam shown in Fig. 7 defines the critical isentrope (vertical lines in Fig. 7) which can be defined for incipient melting (IM), complete melting (CM), and the isentrope which passes through the vapor-liquid critical point (CP). These critical isentropes in the pressure volume plane are plotted in Fig. 8 for ice at 70 and 263K, the range of temperatures appropriate for the surfaces of the Jovian and Saturnian icy satellites. Whereas the isentropes corresponding to IM and CM produced little vapor until

relatively low pressures are achieved, the release isentrope passing through the CP gives rise to ~0.5 mass fraction vapor upon release through the critical point and upon release to pressures below 61 kPa some 0.4 mass fraction is vaporized (Fig. 7).

The critical isentropes of Fig. 8 and Table 5 are also shown in the pressure-particle velocity plane for solid ice in Fig. 2. Examination of where the IM, CM, and CP points fall on the ice Hugoniot (Fig. 2) demonstrates that the minimum infall velocities for ice onto an icy satellite so as to produce melting or vaporization can be specified. Silicate projectiles impacting at greater than 2.1 km/sec or icy projectiles impacting 3.4 km/sec are required to induce IM of ice. CM of ice requires silicate projectiles impacting at least 3 km/sec or ice projectiles impacting at 4.4 km/sec. To obtain 0.4 to 0.5 mass fraction vapor upon passing through the CP requires ~4.5 km/sec for silicate impactors or 7.2 km/sec for pure ice impactors. The latter velocities are in approximate agreement with those of Smoluchowski (1983).

Thus we conclude that although copious melting and vaporization of water ices on icy satellites will occur at meteoroid and cometary impact velocities on the Jovian and Saturnian satellites (Table 3), vaporization processes during accretion will not be significant unless the partial pressure of water is below 61 kPa and the temperature is below 273K during accretion of these objects. We explore the consequences of accretion of the icy satellites in this environment in the next section.

3. ACCRETION OF ICY SATELLITES

We have demonstrated the importance of the existence of low partial pressure of H_2O (below 61 kPa or 6.1 millibar) for vaporization to be important in impact processes during accretion. For accretion under low water partial

pressure conditions and low temperatures, impact vaporization is, however, readily accomplished because the liquid stability field of water is entirely bypassed. Examination of the Mollier diagram of water (Fig. 7) in this low temperature region indicates that an enthalpy gain of 2800 kJ/kg are required to completely vaporize Ice I at pressures below the vapor-liquid ice I triple point. Rather than assume that the Jovian satellites accreted in a gaseous nebula in which the partial pressure of water was at the saturation point at temperatures varying from (150 to 230K) as assumed by Lunine and Stevenson (1982), in the present paper we will examine the consequences of creating icy satellites via infall of planetesimals in a dry, undersaturated environment.

We assume as an extreme case once material is vaporized upon impact, it is lost from the planet. The more complicated problem of precipitation versus thermal loss of H_2O and the general thermal state of the accreting planetary atmosphere is not addressed.

We shall first examine the case of accretion of a pure icy planet at low pressures. If we assume that a porous icy regolith forms in this situation we can model the fraction of ice impact vaporized, f, as being equal to:

$$f = V_i^2 / (2 \cdot \Delta H_{subl}) \qquad (23)$$

where V_i is planetesimal impact velocity.

We conclude that it is most likely that at low temperatures and at undersaturated conditions a porous ice regolith some $\sim 10^0$ to 10^2 km thick would be retained on accreting icy satellites because: (1) Porous regoliths are known to adhere to objects as small as $\sim 10^2$ km diameter asteroids in the case of Phobos and Deimos. (2) At low temperatures ice retains ~50% porosity until overburden lithostatic stresses of ~5 MPa are exerted (Anderson and Benson, 1963).

At any point in the accretion of a uniform density planetary satellite, ρ_0, the minimum infall velocity, $V_{i,min}$ is equal to the escape velocity, V_{esc} which is

$$V_{esc} = \sqrt{8\pi G \rho_0 / 3}\, R \tag{24}$$

where G is the gravitational constant. We now assume that

$$V_i = V_{i,min} = V_{esc} \tag{25}$$

and calculate for a pure water planet how much incident material accreted is retained versus planetary mass (Fig. 9). We observe that at planetary masses of $\sim 10^{24}$g the infall velocity is so slow (0.5 km/sec) that little impact vaporization of H_2O occurs. However, as the pure H_2O satellite accretes in this environment an increasing fraction of the mass delivered is impact vaporized and becomes lost to the object. As can be seen in Fig. 9 when the planet mass is $\sim 10^{26}$g, the minimum infall velocity is ~2 km/sec and only ~0.44 mass fraction of the incident planetesimal material has been retained. For a pure H_2O planet as massive as Titan or Callisto only ~15% of the infalling mass is not impact vaporized.

If now the same calculation is carried out for 0.4 mass fraction of silicate, 0.6 mass fraction water, planetesimals typical of material condensing from the primordial Jovian and Saturnian nebulae, and, we assume a silicate density of 3.0 Mg/m^3 for the silicate fraction, the water vaporization is less extreme as also indicated in Fig. 9. Planetesimals with this composition when accreting to form a planet retain ~65% of the incident mass for an object when the object becomes massive as Titan or Ganymede.

We sought to examine the question of whether accretion of a water-silicate mixture, initial density 1.27 Mg/m^3 which approximates the mean density of the smaller satellites (Mimas, Enseladus, Tethys, Dione, Iapetus and Rhea) results in

sufficient impact vaporization to obtain a mean density of >1.8 Mg/m^3 corresponding to larger satellites Callisto, Titan, and Ganymede. As indicated in Fig. 10 accretion of such a mixture results in a mean planetary density of only ~1.5 Mg/m^3. Moreover, also shown in Fig. 10, the situation is not especially improved if one assumes a 10^3 km silicate core for the larger satellites. In this case the increase in the average final density is only slight. The interesting minimum density at 1.55 Mg/m^3 is caused by the process of initially reducing the mean density of the growing planet with a silicate core by accreting water-bearing material. However, as the planet grows, an increasing fraction of the water-bearing material contributed is shock-vaporized and lost, and finally at a radius of ~2300 km the mean density begins to increase again. We conclude from these calculations that the simple process of impact vaporization in a regolith and a loss of all the shock volatilized water cannot make planets with densities as high as Callisto, Titan, and Ganymede from a protosolar mixture of 60% (mass) water and 40% silicate which both correspond to a primordial water silicate mixture as well as approximates the average density of the smaller satellites of Saturn. As indicated in Fig. 10 if one relaxes the constraint on the planetary composition slightly, and assume 43% H_2O and 57% silicate, it is possible to produce objects with exactly the density of Callisto, Titan, and Ganymede (which correspond to ~40% water and 60% silicate) by the impact volatilization process outlined above. Finally, if instead of assuming a porous regolith, we make a slightly more drastic assumption and assume porous planetesimals (and restrict impact vaporization to the mass of planetesimal material only) it is possible to slightly enhance the impact volatilization process to achieve objects close to the radius of Callisto, Titan, and Ganymede with material very close to the mean density of the smaller satellites of Saturn. In this case our calculations demonstrate that starting with 54% H_2O and 46% silicate composition

(starting density 1.35 Mg/m^3) planets having the Ganymede radius of 2600 km and a density of 1.85 to 1.9 can be achieved.

The present results suggest that impact volatilization can give rise to the greater density of the larger Jovian and Saturnian satellites as a result of vaporization of porous, water, ice, and possibly also NH_3 ice during accretion and all but the essentially silicate satellites can have accreted from the same primordial solar composition material. The final density of Jovian and Saturnian satellites then may just be the consequence of the amount of material in orbit around Jupiter and Saturn at a particular radius, and hence, ultimate satellite size.

4. SUMMARY AND CONCLUSIONS

Shock wave data for polycrystalline, porous ice, and liquid water are available over a sufficiently wide range of pressure. The peak shock state achieved upon accretionary impacts up to 2.6 km/sec, as well as, impacts of 20-30 km/sec for cometary encounters are described using the impedance match method. A key calculation to determine the intersection of the pressure-volume-temperature-energy isentrope with the Hugoniot curve of water and ice so as to determine the entropy function along the Hugoniot. Knowledge of the entropy gain along the Hugoniot of ice determines whether upon rarefaction from a peak shock pressure will result in incipient melting, complete melting, or partial vaporization. The latter will occur upon passage of the isentropes through thermodynamic states near the vapor-liquid critical point (at 64 K, 221 MPa and 3.1 m^3/Mg). For ice the shock pressure required to induce incipient melting is 6 GPa, complete melting is 10 GPa, and passage through the vapor-liquid critical point is 22.5 GPa. These pressure values depend only slightly on the initial temperature of the water-ice. Upon isentropic release along the isentrope passing through the critical point, the mean fraction of water vaporized is ~0.5 which decreases to 0.4 upon cooling and expansion to below the vapor-liquid-ice I triple point.

The vapor-liquid-ice I triple point at 61.08 kPa (6.1 mbar) and 273 K occurs at a point where the condensed phase density is 1 Mg/m^3 and the vapor phase density is 5×10^{-6} Mg/m^3 plays an important role in impact vaporization in an environment with low partial pressure of H_2O. The minimum impact velocity onto an icy satellite surface required to induce the incipient melting is 2.1 and 3.4 km/sec for silicate and icy projectiles, respectively. Complete melting of ice requires silicate or icy impactors traveling at ~3 and 4.4 km/sec, respectively. To obtain 0.4 to 0.5 mass fraction vapor upon passing through the liquid-vapor

critical point requires 4.5 to 7.2 km/sec impact velocities for silicate and ice projectiles, respectively.

The Rice-Walsh-Bakanova equation of state in which internal energy or enthalpy is specified along a pressure-volume reference curve can be used to calculate other thermodynamic states such as along isentropes, at the same pressure, for different volumes and temperatures from the thermodynamic parameters $(\partial H/\partial V)_P$ or $P(\partial V/\partial E)_P$. These parameters which are assumed to be only a function of P are fit to the singly or doubly shocked Hugoniot data for water, ice, and porous ice.

The satellites of Jupiter and Saturn are classified into three groups according to density. The inner, silicate, satellites of Jupiter (Amalthea, Io, and Europa) the partially devolatilized (pd) satellites (Ganymede, Callisto, and Titan), and the smaller primordial (p) satellites (Mimas, Enseladus, Tethys, Dione, Rhea, and Iapetus). The latter two groups have mean densities of 1.8 to 1.9 Mg/m^3 and 1.0 to 1.4 Mg/m^3. We infer that the densities of the P group also correspond to the densities of the particles in the rings of Saturn and Jupiter. We suggest that the p satellites are composed largely of primordial solar ratio material controlled by the oxygen/silicon ratio (15.5) and the oxygen/magnesium ratio (17.4) of the primitive Jovian and Saturnian nebulae. The primordial solar ratios, if these correspond to objects having silicate and water ice compositions, would have densities of 1.1 to 1.2 Mg/m^3. We have examined the hypothesis that the large pd satellites achieved their higher densities (1.8 to 1.9 Mg/m^3) upon partial impact devolatilization during accretion starting with planetesimals of material similar in density, 1.27 Mg/m^3, (60% ice, 40% silicate) to that of the smaller satellites. Accretion of planetesimals of such a composition assuming impact volatilization at partial pressures of H_2O below 62 kPa in a porous regolith yields Ganymedean-sized planets with mean planetary

densities of only 1.5 Mg/m^3. However, starting with planetesimals having densities of 1.62 Mg/m^3 (43% H_2O and 57% silicate) give rise to mean satellite densities of 1.9 Mg/m^3 for Ganymedean-sized objects.

If impact volatilization of initially porous planetesimals is assumed our calculations demonstrate that starting with planetesimals of composition 54% H_2O and 46% silicate (mean density 1.35 Mg/m^3) and partial devolatilization during accretion occurs leads to objects having a Ganymedean radius of 2600 km and a mean density of 1.85 Mg/m^3.

The present results suggest a mechanism for the formation processes of the higher density partially devolatilized, satellites of Saturn and Jupiter. The accretion devolatilization process depends on the relative amount of material present in different zones orbiting in the nebular around each proto-planet and less on the assumed mean radial temperature at a given distance from the planet.

Acknowledgments. Research supported under NASA grants NSG 7129 and NAGW-205. We have profitted from the previous work of Mark Morley who first looked at the accretion problem from a different perspective, as well as the technical discussions with D. Stevenson and J. Lunine. We are grateful to A. Dollfus and R. Smoluchowski for inviting us to present this paper to a critical audience in Nice, France. Contribution #4107, of the Division of Geological and Planetary Sciences, California Institute of Technology, Pasadena, California.

APPENDIX A. SHOCK TEMPERATURES AND THE WATER EQUATION OF STATE

A stringent test of the complete thermal equation of state for fluids such as water are to compare predicted sound speeds and Hugoniot temperatures to measurements. Previously Bakanova et al. (1976) very favorably compared their predicted sound velocity along the water Hugoniot with measurements to ~60 GPa. Shock temperatures were also calculated and compared with previous relatively low pressure data of Kormer (1968). Other work by Lyzenga and Ahrens (1980), Lyzenga et al. (1983a,b), Ahrens et al. (1982), Nellis et al. (1984), and Boslough et al. (1984) for a variety of solids and fluids demonstrate that upon comparing calculated and measured shock temperature T_H versus shock pressure, P, the absolute value of T_H at a given pressure was very sensitive to the total energy budget of the material (e.g. occurrence of phase changes) whereas a slope of the P versus T_H relation is sensitive to specific heat.

In Fig. 1A the available H_2O shock temperature data of Kormer (1968) and the more recent higher temperature and pressure data of Lyzenga et al. (1982) are shown relative to previous shock temperature calculations. As is evident from the figure, the calculation of Ree based on a repulsive parameter equation of state which does not take into account, the already mentioned, extensive pressure-induced ionization (Mitchell and Nellis, 1982) yields temperatures which are too high by ~600K, especially at higher pressures (above 50 GPa). Rice and Walsh's calculations are too high largely because the data range they studied, up to ~25 GPa, did not encompass as much of the higher pressure range where subsequent measurements demonstrate that the Hugoniot curve is more compressive (especially above 30 GPa) (Mitchell and Nellis, 1982) than would be anticipated from simple extrapolation of the lower pressure data. Both the curve labeled Cowperthwaite and Shaw (1970) and a present calculations agree well with Kormer's 1968 lower pressure results. Cowperthwaite and Shaw (1970)

use a thermal equation of state which was derived from a careful fit to the lower pressure thermodynamic data, and took into account the strong temperature dependence of specific heat at constant volume. For the present calculation curve we employed the form of the Bakanova equation of state and used equation 21 for specifying $\eta = P/(\partial V/\partial E)_P$ as a function of P. Instead of using a theoretical value of E_{io}, T_{io}, and V_{io} to specify the foot of a series of isentropes at P_{io} = 1 GPa in the low temperature and high pressure regime as do Bakanova et al. (1976), we used the experimentally based thermodynamic and equation of state data specified in Table 1A. Hence it is not surprising that our results agree so closely with those of Cowperthwaite and Shaw (1970). Finally we note that over the range from 65 to 80 GPa the Bakanova et al. (1976) equation of state is in excellent agreement with the recently measured shock temperatures. We thus conclude that this form of this equation of state provides an accurate description of the properties of shocked water and presumably ice up to 50 GPa when constrained by the thermodynamic data extending to ~1 GPa and ~1273K. At higher pressures > 50 GPa the theoretical description of the high temperature - low pressure properties of water proffered by Bakanova et al. (1976) fits both the shock temperature data, the sound speed, and the reflected shock, and porous ice data.

REFERENCES

Ahrens, T.J., Lyzenga, G.A., and Mitchell, A.C. 1982, in *High Pressure Research in Geophysics*, ed. by S. Akimoto and M.H. Manghnani, Center for Academic Publications, Japan, pp. 579-594.

Ahrens, T.J. and O'Keefe, J.D. 1972, The Moon 4, pp. 214-249.

Anderson, D.L. and Benson, C.S. 1963, in *Ice and Snow*, ed. by W.D. Kingery, MIT Press, pp. 391-411.

Anderson, G.D. 1968, U.S. Army CRREL Res. Rept. 257.

Bakanova, A.A., Zubarev, V.N., Sutulov, Yu.N., and Trunin, R.F. 1976, Sov. Phys. JETP. 41, pp. 544.

Boslough, M.B., Ahrens, T.J., and Mitchell, A.C. 1984, J. Geophys. Res., in press.

Bosnjakov, F., Renz, U., Burow, P. 1970, *Mollier Enthalpy, Entropy Diagram of Water*, GZH, Zagreb, Hemisphere Publishing Corp., Washington, D.C.

Burnham, C.W., Holloway, J.R., and Davis, N.F. 1969, The Geological Society of America special paper #132, 99 pp.

Cole, G.H.A. 1984, Quant. J. Roy. astr. Soc. 25, pp. 19-27.

Cowperthwaite, M. and Shaw, R. 1970, J. Chem. Phys. 53, pp. 555-560.

Dorsey, N.E. 1940, *Properties of Ordinary Water-Substance*, Reinhold Publ. Corp., N.Y., 673 pp.

Fletcher, N.H. 1970, *The Chemical Physics of Ice*, Cambridge Univ. Press, 271 pp.

Gaffney, E.S. 1984, Proc. NATO Workshop on Ices in the Solar System, Nice, France, Jan 16-19, 1984.

Gaffney, E.S. and Ahrens, T.J. 1980, Geophys. Res. Lett. 7, pp. 407-409.

Kormer, S.B. 1968, Sov. Phys. Usp. 11, pp. 229-254.

Larson, D.B., Bearson, G.D., and Taylor, J.R. 1973, *No. Amer. Contrib. 2nd Int. Conf. Permafrost, Yakutsk*, pp. 318-325.

Lunine, J.A. and Stevenson, D.J. 1982, Icarus 52, pp. 14-39.

Lyzenga, G.A., Ahrens, T.J., Nellis, W.J., and Mitchell, A.C. 1982, J. Chem. Phys. 76, pp. 6282-6286.

Lyzenga, G.A. and Ahrens, T.J. 1980, Geophys. Res. Lett. 7, pp. 141-144.

McQueen, R.G., Marsh, S.P., Taylor, J.W., Fritz, J.N., and Carter, W.J. 1970, in *High Velocity Impact Phenomena*, ed. by Kinslow, R., Academic Press, New York, pp. 294-419.

Marsh, S.P. 1980, LASL Shock Hugoniot Data, University of California Press, Berkeley, pp. 327.

Mitchell, A.C. and Nellis, W.J. 1982, J. Chem. Phys. 76, pp. 6273-6281.

Morrison, D. 1982, in *Satellites of Jupiter*, ed. by D. Morrison, U. Ariz. Press, Tucson, pp. 3-43.

Nellis, W.J., Ree, F.H., Trainor, R.J., Mitchell, A.C., and Boslough, M.B. 1984, J. Chem. Phys. 80, pp. 2789-.

Pollack, J.B. and Fanale, F. 1982, in *Satellites of Jupiter*, ed. by D. Morrison, Univ. Ariz., Tucson, pp. 872-910.

Pollack, J.B. and Reynolds, R.T. 1974, Icarus 21, pp. 248-253.

O'Keefe, J.D. and Ahrens, T.J. 1977, Proc. Lunar Sci. Conf. 8th, pp. 3357-3374.

Ree, F.H. 1982, J. Chem. Phys. 76, pp. 6287-6302.

Rice, M.H., McQueen, R.G., and Walsh, J.M. 1958, Solid State Phys. 6, pp. 1-63.

Rice, M.H. and Walsh, J.M. 1957, J. Chem. Phys. 26, pp. 824-830.

Ross, J.E. and Aller, L.H. 1976, Science 191, pp. 1223-1229.

Smith, B.A., Soderblom, L.A., Johnson, T.V., Ingersoll, A.P., Collins, S.A., Shoemaker, E.M., Hunt, G.E., Masursky, H., Carr, M.H., Davies, M.E., Cook, A.F. II, Boyce, J., Danielson, G.E., Owen, T., Sagan, C., Beebe, R.F., Veverka, J., Strom, R.G., McCauley, J.F., Morrison, D., Briggs, G.A., and Suomi, V.E. 1979a, Science 204, pp. 945-972.

Smith, B.F., Soderblom, L.A., Beebe, R., Boyce, J., Briggs, G., Carr, M., Collins, S.A., Cook, A.F., Danielson, G.E., Davies, M.E., Hunt, G.E., Ingersoll, A., Johnson, T.V., McCauly, J., Masursky, H., Owen, T., Sagan, C., Shoemaker, E.M., Strom, S., Suomi, V.E., and Veverka, J. 1979b, Science 206, pp. 927-950.

Smith, B.F., Soderblom, L.A, Beebe, R., Boyce, J., Briggs, G., Bunker, A., Collins, S.A., Hansen, C.F., Johnson, T.V., Mitchell, J.L., Terrille, R.J., Carr, M., Cook, A.F., Cuzzi, J., Pollack, J.B., Danielson, G.E., Ingersoll, A., Davies, M.E., Hunt, G., Masursky, H., Shoemaker, E.M., Morrison, D., Owen, T., Sagan, C., Veverka, J., Strom, J., Suomi, V.E. 1981, Science 212, pp. 163-191.

Smoluchowski, R. 1983, Science 222, pp. 161-163.

Stone, E.C. and Miner, E.D. 1982, Science 215, pp. 499-504.

Walsh, J.M. and Rice, M.H. 1957, J. Chem. Phys. 26, pp. 815-823.

Weast, R.C. 1982, *CRC Handbook of Chemistry and Physics*, 63rd Ed., Chemical Publ. Co., Cleveland.

Figure 1. Mean orbital radius versus satellite density for the Jovian and Saturnian systems.

Figure 2. Shock velocity versus particle velocity for ice at 258 and 263 K.

Figure 3. Shock pressure versus particle velocity for water, ice, and porous ice. Curve for serpentinite, representative of planetary silicates after Marsh (1980). Escape velocity for satellites and planets indicated along the particle velocity axis. Shock pressures required for incipient melting (IM), complete melting (CM), and the critical point isentrope (CP) for ice are indicated.

Figure 4. Bakanova parameter, versus, pressure.

Figure 5. Principal Hugoniot and release isentropes for water in the pressure specific volume plane after Bakanova et al. (1976).

Figure 6. Log_{10} pressure (GPa) versus temperature phase diagram for H_2O. Hugoniot for ice and liquid water and release isentrope passing through liquid-vapor critical point (K) and water-vapor-ice I, triple point (CP) is indicated.

Figure 7. Simplified Mollier enthalpy entropy diagram of water, after Bosnjakovic, Renz, and Burow (1970).

Figure 8. Hugoniot for ice centered at 70 and 263 K and release isentropes for incipient melting (IM), complete melting (CM), and critical point (CP) isentropes in pressure volume plane. Hugoniot of ice centered at 70 K inferred from thermal expansion data for ice collected in Fletcher (1970).

Figure 9. Mass fraction of incident planetesimal material accreted, versus, planetary mass for pure H_2O and 0.4 silicate + 0.6 H_2O planet. A porous, ideal locking solid (similar to snow) is assumed on the surface of the growing planet. All the gravitational energy of accretion is deposited in this layer and gives rise to partial vaporization of ice at temperatures below 273.16 K and 61.08 kPa (6.108 mbar).

Figure 10. Average uncompressed density of an icy planet versus planetary radius. Light curves are for accretion of solid planetesimals and a regolith-covered planet. Heavy curve is for accretion of porous planetesimals and a solid planetary surface.

Figure 1A. Shock temperature versus shock pressure. Theoretical calculations and experimental measurements.

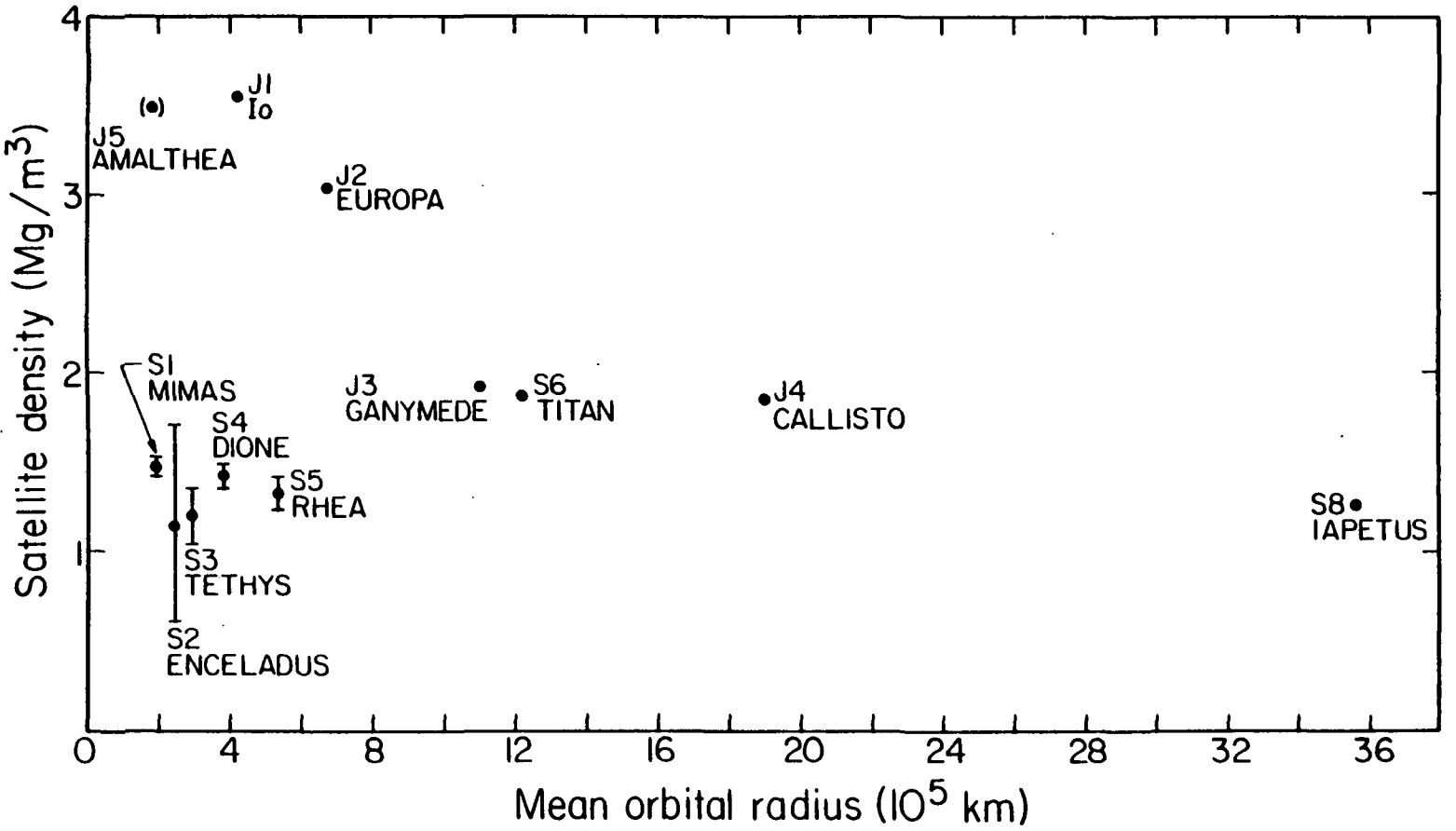

(1)

TJA84086SST

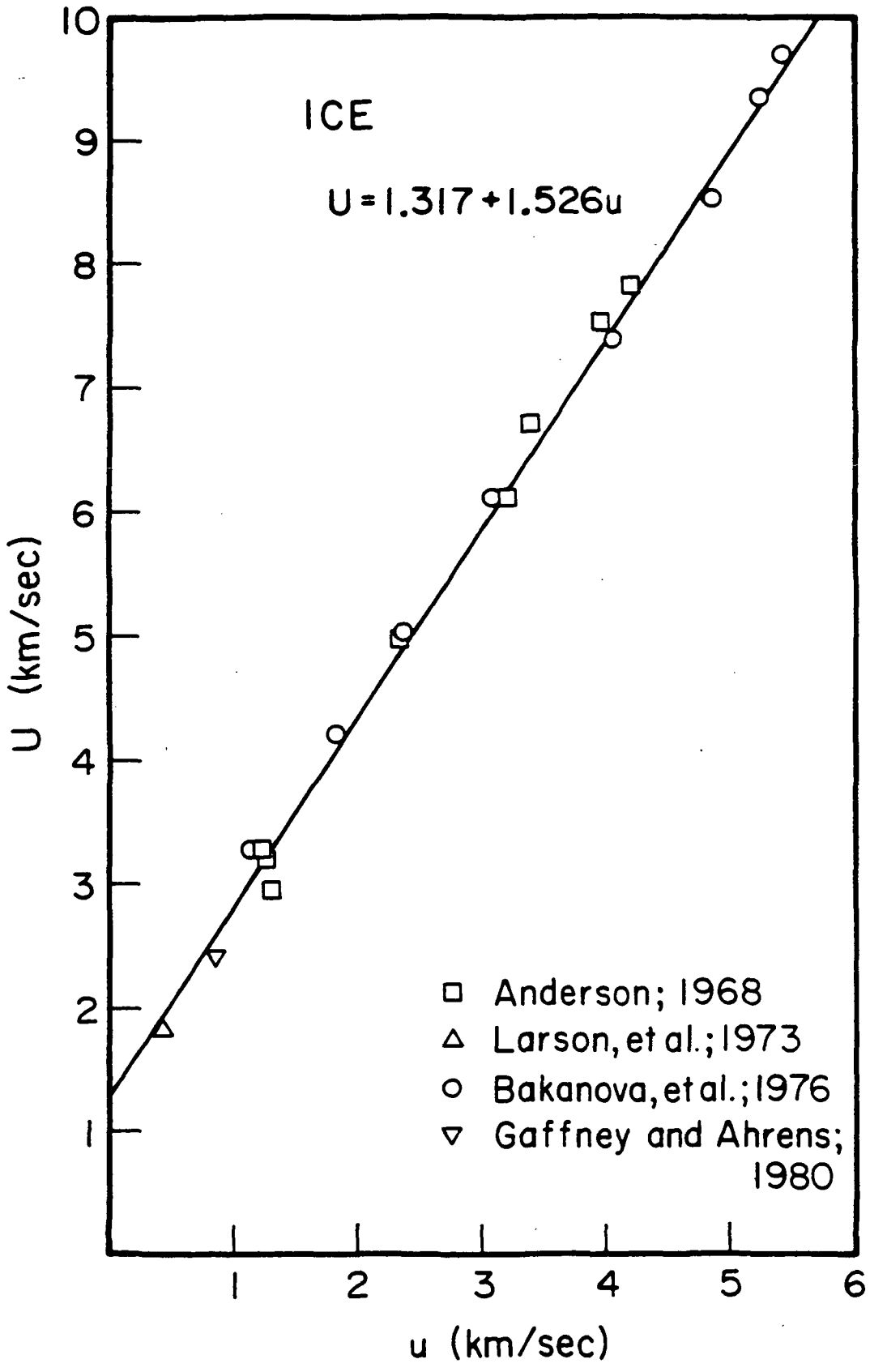

TJA84087SFD

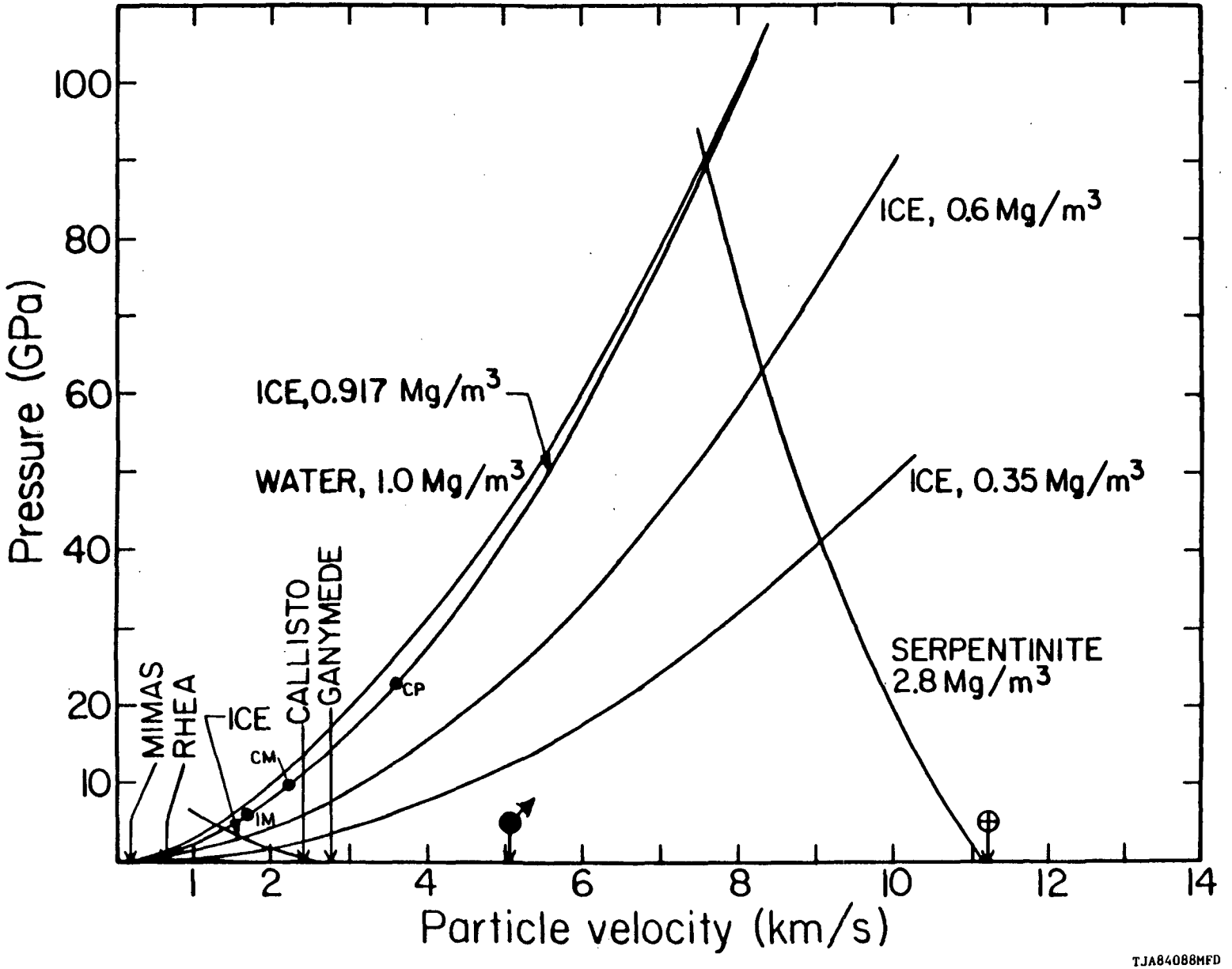
Pressure (GPa)
100
80
60
40
20
10
1
2
4
6
8
10
12
14
Particle velocity (km/s)
ICE, 0.6 Mg/m3
ICE, 0.917 Mg/m3
WATER, 1.0 Mg/m3
ICE, 0.35 Mg/m3
SERPENTINITE
2.8 Mg/m3
MIMAS
RHEA
ICE
CALLISTO
GANYMEDE
CP
CM
IM
TJA84088MFD

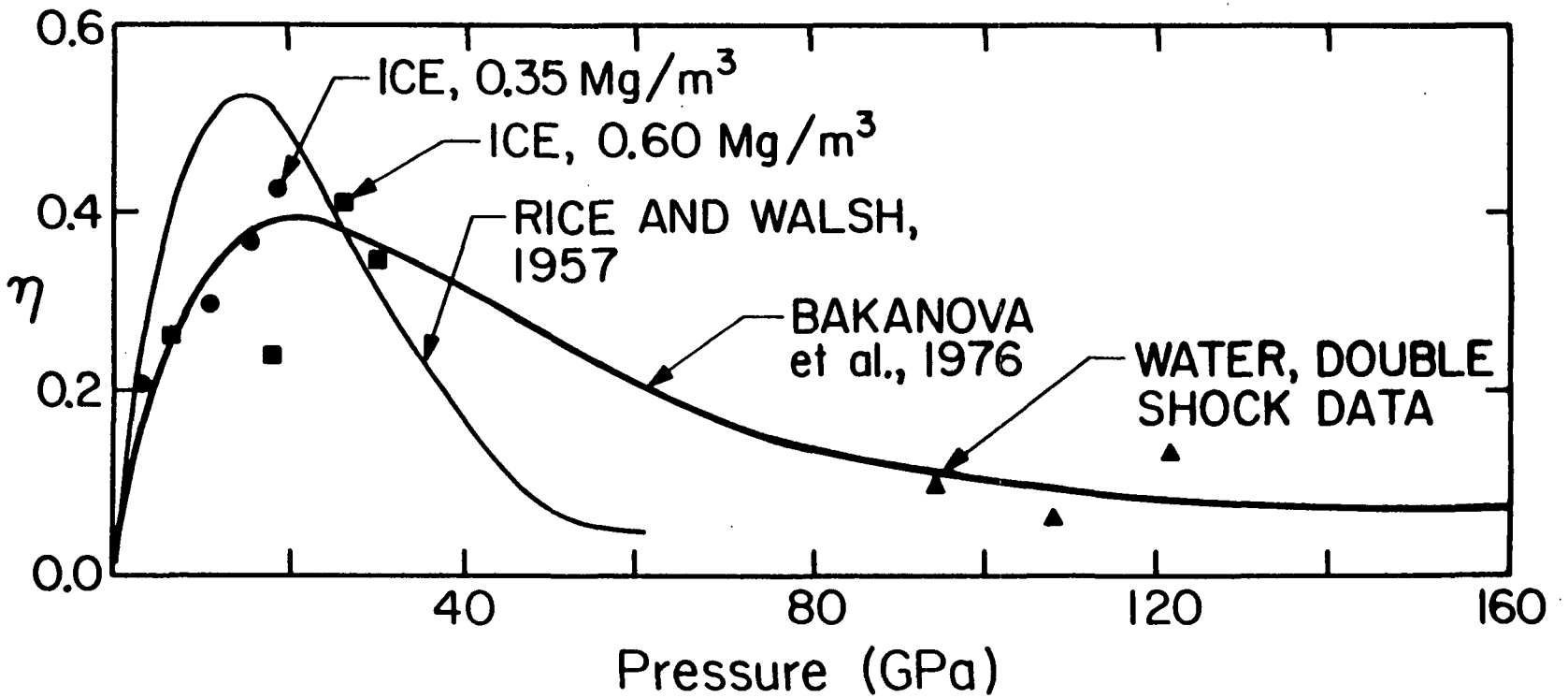

TJA84089SFD

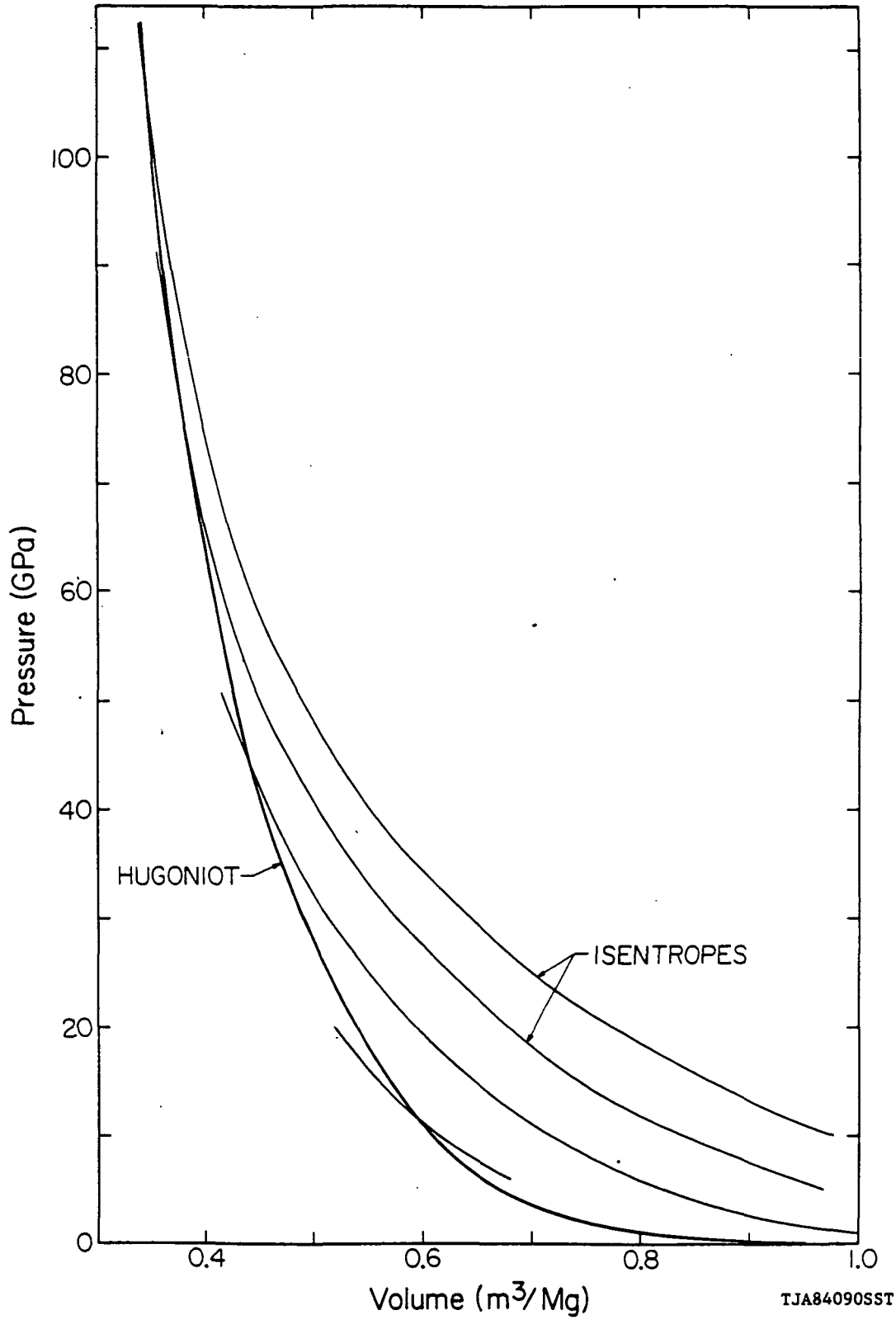
Pressure (GPa)
100
80
60
40
20
0
0.4
0.6
0.8
1.0
Volume (m3/Mg)
HUGONIOT
ISENTROPES
TJA84090SST

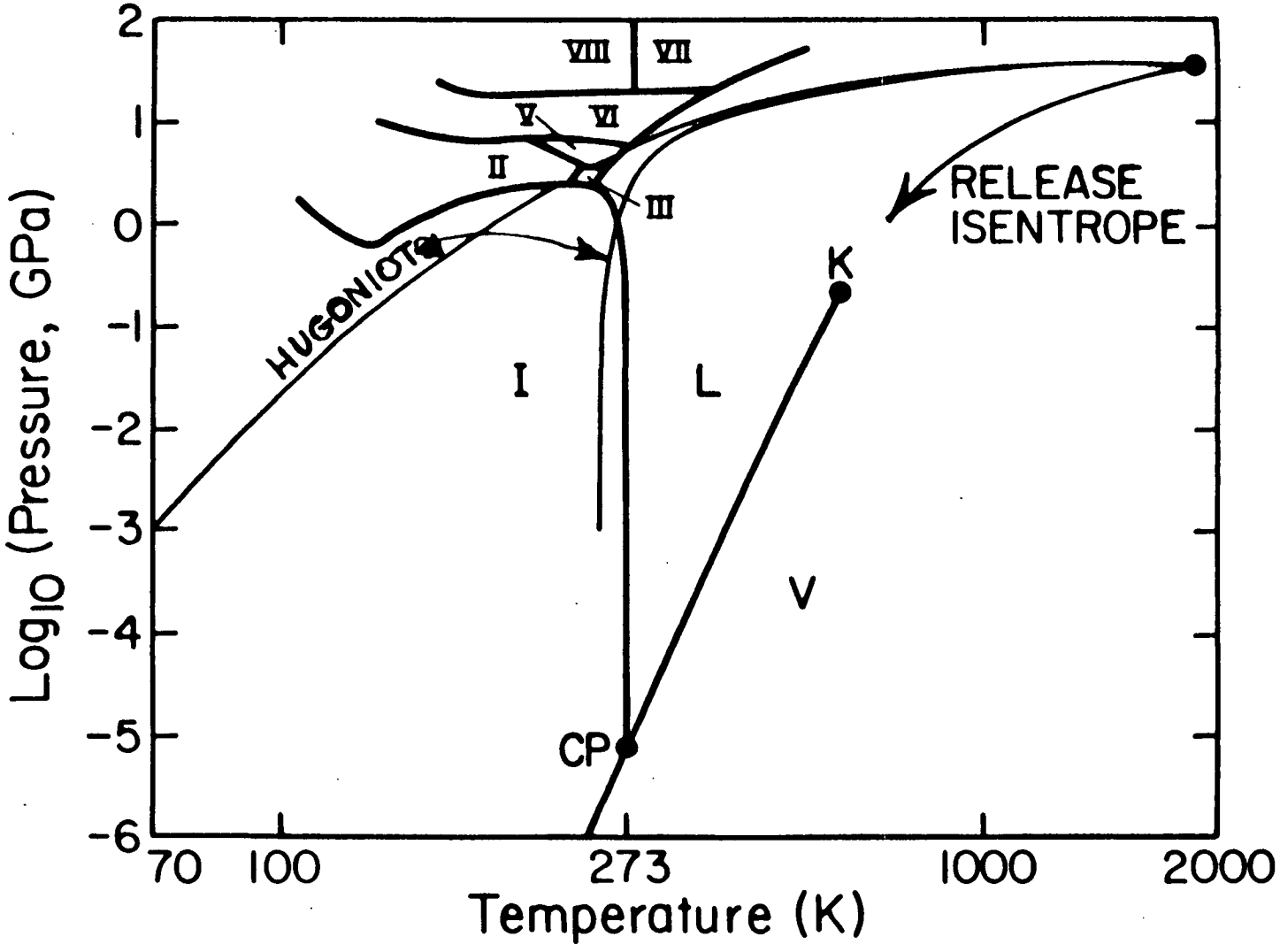
2
1
0
-1
-2
-3
-4
-5
-6
Log10 (Pressure, GPa)
70
100
273
1000
2000
Temperature (K)
VIII
VII
V
VI
II
III
HUGONIOT
RELEASE
ISENTROPE
K
I
L
V
CP

TJA8409

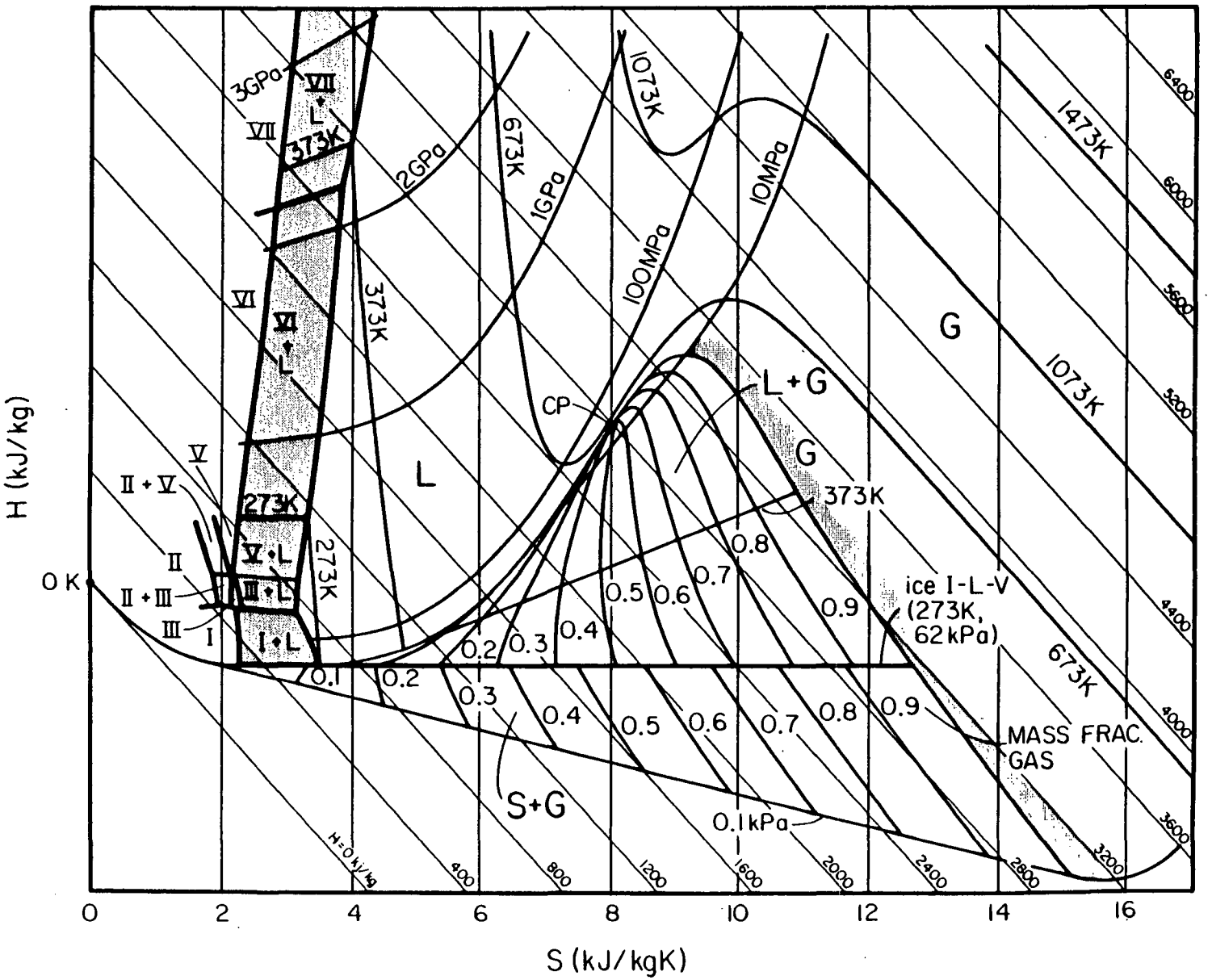

TJA84092MST

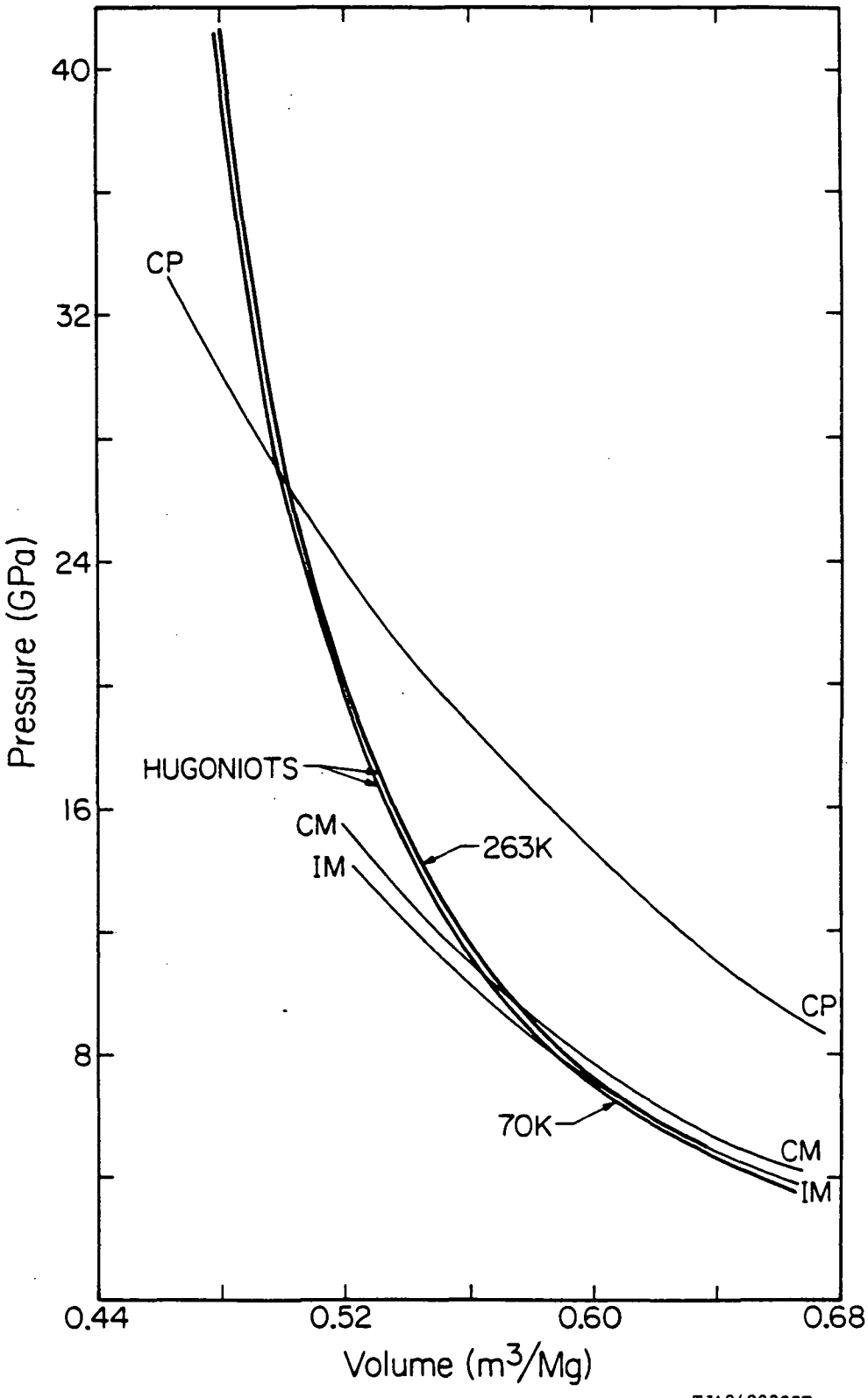

TJA84093SST

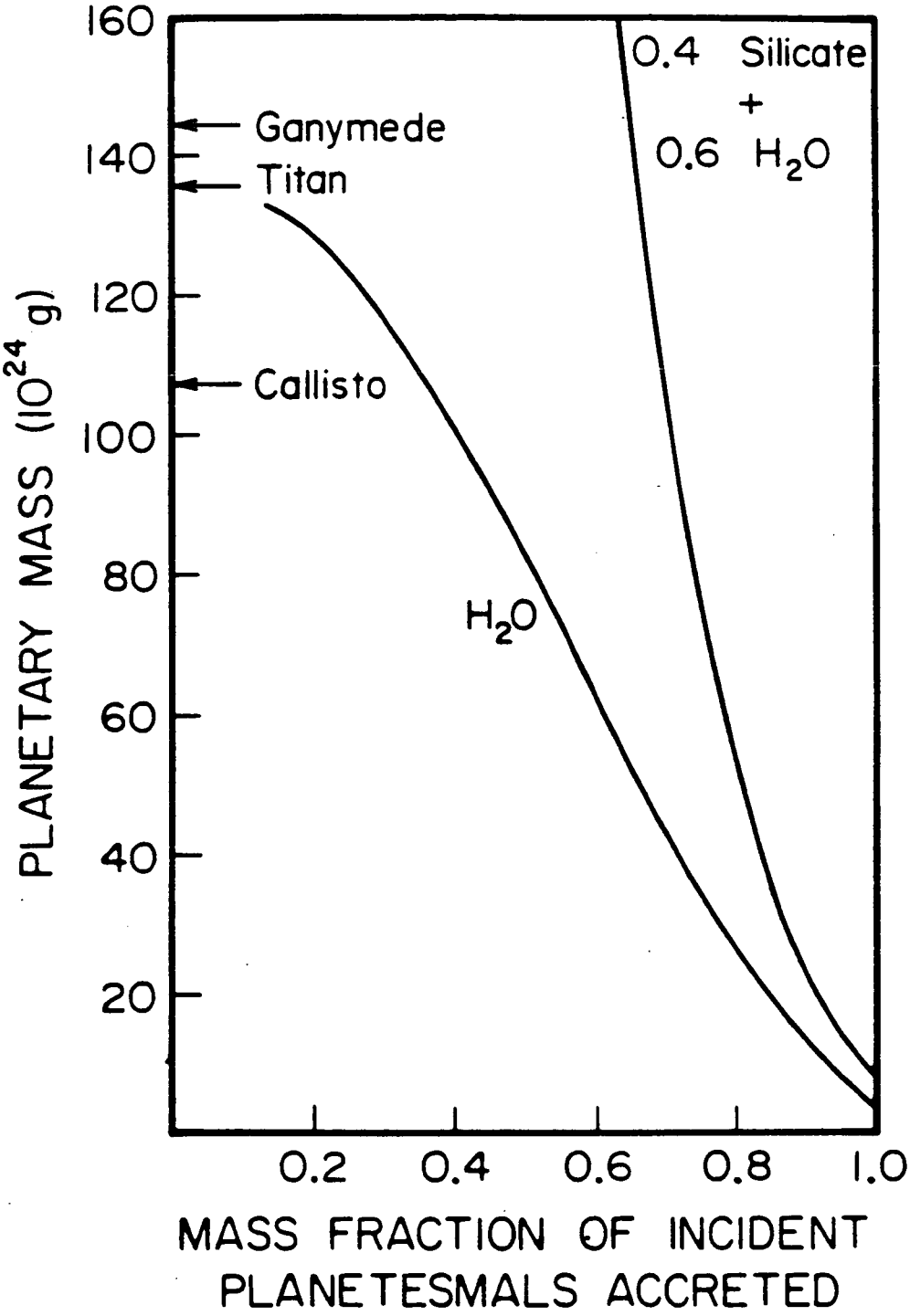

TJA84001SFD

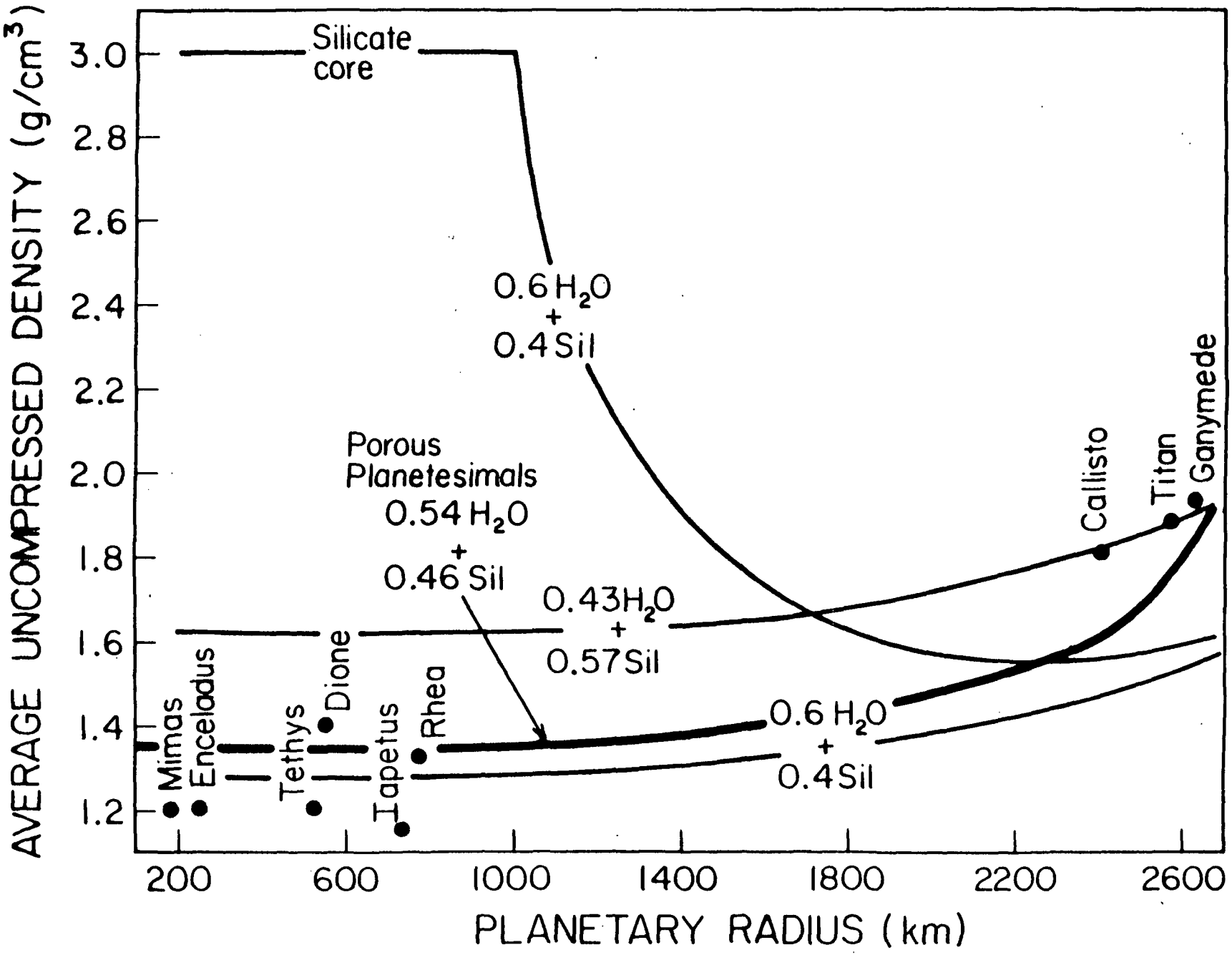
AVERAGE UNCOMPRESSED DENSITY (g/cm³)
3.0
2.8
2.6
2.4
2.2
2.0
1.8
1.6
1.4
1.2
Silicate core
0.6 H₂O + 0.4 Sil
Porous Planetesimals
0.54 H₂O + 0.46 Sil
0.43 H₂O + 0.57 Sil
0.6 H₂O + 0.4 Sil
Callisto
Titan
Ganymede
Mimas
Enceladus
Tethys
Dione
Tapetus
Rhea
200
600
1000
1400
1800
2200
2600
PLANETARY RADIUS (km)

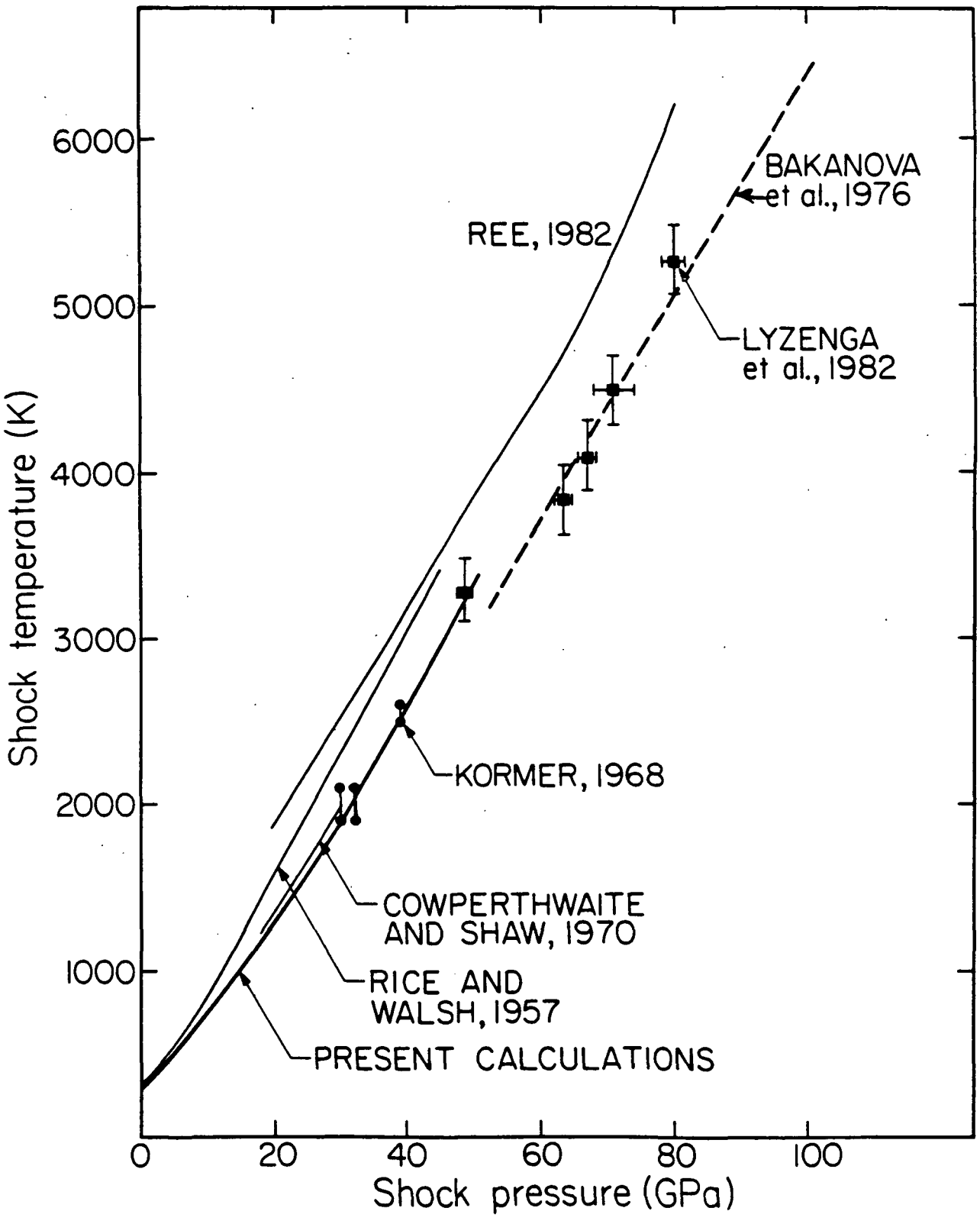

TJA84094SST

1A

Table 1. Characteristics of Major Jovian and Saturnian Satellites[a]

Satellite	Mean Orbital Radius (10^5km)	Radius (km)	Mass (10^{20}kg)	Mean Density (Mg/m^3)	Satellite Class.
J-5 Amalthea	1.8	(96)	(0.13)	(3.5)	(silicate)
J1-Io	4.2	1815±10	892	3.55	silicate
J2-Europa	6.7	1569±10	487	3.04	silicate
J3-Ganymede	11	2631±10	1490	1.93	p.d.
J4-Callisto	19	2400±10	1075	1.83	p.d.
S1-Mimas	1.9	195±5	0.37	1.44±0.18	p
S2-Enceladus	2.4	250±10	0.72	1.16±0.55	p
S3-Tethys	2.9	525±10	6.06	1.21±0.16	p
S4-Dione	3.8	560±10	10.30	1.43±0.06	p
S5-Rhea	5.3	765±10	24.38	1.33±0.09	p
S6-Titan	12.2	2560±26	1335.25	1.88±0.01	p.d.
S8-Iapetus	35.6	720±20	18.76	1.16±.09	p

[a] Data compiled from Morrison (1982), Stone and Miner (1982), Lunine and Stevenson (1982).

Table 2. Shock-Particle Velocity Data for Water, Ice, and Porous Ice

Initial Material	Initial Density (Mg/m^3)	C_o (km/sec)	λ_1	λ_2 (sec/km)	Range of u (km/sec)	Ref.
Water (294-298K)	0.9979±0.0004	2.393	1.333	-	1.5<u<7.1	(a)
Water (293)	0.99823[b]	1.50	2.0	-0.107	0<u<4.0	(c)
Water (293)	0.99823[b]	3.2	1.144	-	u>4.0	(c)
Ice (258)	0.915	1.57	1.465	-		(c)
Ice (263)	0.9230[b]	1.317	1.526	-		(d)
Porous Ice (258)	0.60	0.74	1.425	-		(c)
Porous Ice (258)	0.35	0.0	1.425	-		(c)

[a] Mitchell and Nellis (1982)

[b] Nominal value Weast (1982)

[c] Bakanova et al. (1976)

[d] present fit to 18 data points (8 data, Bakanova et al., 1976; 8 data, Anderson, 1988; 1 point, Larsen et al., 1972; 1 point, Ahrens and Gaffney, 1976).

Table 3. Relative cratering rates on the Galilean satellites for mean encounter velocity of 8 km/sec (Smith et al., 1979b)

Satellite	Flux concentration factor by Jupiter gravity	Mean Impact Velocity (km/sec)	Relative Crater Production Rate
Callisto	3.3	14	1
Ganymede	5.0	18	2.0
Europa	7.3	21	2.8
Io	11.1	26	5.3

Table 4. Critical Isentropes in the Water System

Critical Isentrope	Determining State	Entropy* (kJ/kgK)	State at 1 GPa				
			Phase	Temperature (K)	Enthalpy* (kJ/kg)	Volume (Mg/m^3)	Internal Energy (kJ/kg)
Incipient Melting (IM)	Triple Point Ice III-Ice V-Liquid	2.21	Ice VI	400	1140	0.735	405
Complete Melting (CM)	Triple Point Ice I-Ice III-Liquid	3.16	Ice VI+ Liquid	400	1400	0.736	614
Liquid-Vapor Critical Point (CP)	Liquid-Vapor	7.95	Liquid	1017	4080	1.085	2995
1 GPa and 1273K	none	8.76	Vapor	1273	5022	1.2532	3769

* referenced to 1 bar and 0K

Table 5. Critical Release States, Ice Hugoniots

		70K			263K		
Isentrope Entropy[a]	(kJ/kgK)	T(K)	P(GPa)	V(m^3/Mg)	T(K)	P(GPa)	V(m^3/Mg)
IM	2.21	378	7.6	0.594	363	6.2	0.616
CM	3.16	410	10.8	0.562	298	9.6	0.576
CP	7.95	1756	25.5	0.509	1779	26.7	0.500

(a) referenced to 1 bar and 0K

Table 1A. Shock Temperature, Liquid Water

Isentropic Centered State, 1 GPa			Hugoniot State			
E(kJ/kg	V(m^3/Mg)	T(K)	E(kJ/kg)	V(m^3/Mg)	T(K)	P(GPa)
3166[a]	1.11[a]	1073[a]	8766	0.484	1964	31.5
3769[b]	1.25[b]	1273[b]	10,987	0.460	2447	37.9
(c)	0.868[d]	428[d]	(c)	0.595	584	10.8
(c)	1.014[d]	1286[d]	(c)	0.443	2555	44
(c)	1.19[d]	2143[d]	(c)	0.382	4703	75
(c)	1.381[d]	3000[d]	(c)	0.344	6859	107.4

(a) Bosnjakovic et al., 1970
(b) from Burnham et al., 1969
(c) not calculated
(d) Bakanova et al., 1976